MIPAS measurements of upper tropospheric C2H6 and O3 during the Southern hemispheric biomass burning season in 2003

T. von Clarmann, N. Glatthor, G. P. Stiller, U. Grabowski, M. Höpfner, S. Kellmann, A. Linden, M. Milz, T. Steck, H. Fischer, et al.

Atmos. Chem. Phys. Discuss., 7, 12067–12095, 2007
www.atmos-chem-phys-discuss.net/7/12067/2007/

Atmospheric Chemistry and Physics Discussions

MIPAS measurements of upper tropospheric C_2H_6 and O_3 during the Southern hemispheric biomass burning season in 2003

T. von Clarmann[1], N. Glatthor[1], G. P. Stiller[1], U. Grabowski[1], M. Höpfner[1], S. Kellmann[1], A. Linden[1], M. Milz[1,*], T. Steck[1], H. Fischer[1], B. Funke[2], and M. E. Koukouli[3]

[1]Forschungszentrum Karlsruhe, Institut für Meteorologie und Klimaforschung, Karlsruhe, Germany
[2]Instituto de Astrofísica de Andalucía CSIC, Granada, Spain
[3]Laboratory of Atmospheric Physics, Physics Department, Aristotle University of Thessaloniki, Thessaloniki, Greece
[*]now at: Institutionen för Rymdvetenskap, Luleå Tekniska Universitet, Kiruna, Sweden

Received: 26 July 2007 – Accepted: 8 August 2007 – Published: 15 August 2007

Correspondence to: T. von Clarmann (thomas.clarmann@imk.fzk.de)

Abstract

Under cloud free conditions, the Michelson Interferometer for Passive Atmospheric Sounding (MIPAS) provides measurements of spectrally resolved limb radiances down to the upper troposphere. These are used to infer global distributions of mixing ratios of atmospheric constituents in the upper troposphere and the stratosphere. From 21 October to 14 November 2003, MIPAS observed enhanced amounts of upper tropospheric C_2H_6 (up to about 400 pptv, depending on spectroscopic data chosen) and ozone (up to about 80 ppbv). By means of trajectory calculations, the enhancements observed in the Southern hemisphere are, at least partly, attributed to a biomass burning plume, which covers wide parts of the Southern hemisphere, from South America, the Atlantic ocean, Africa, the Indian Ocean to Australia. The chemical composition of the part of the plume-like pollution belt associated with South American rainforest burning appears different from the part associated with Southern African savanna burning. In particular, African savanna fires lead to a larger ozone enhancement than South American rainforest fires.

1 Introduction

Long-lived products of biomass burning are intercontinentally transported and form large plumes which are visible over months. The Atmospheric Chemistry Experiment (ACE) has measured CO, C_2H_6, HCN and C_2H_2 during the 2004 Southern hemispheric biomass burning season (Rinsland et al., 2005; Coheur et al., 2007). The Measurements Of Pollution In The Troposphere (MOPITT) experiment has provided evidence of enhanced tropospheric CO during the 2003 Southern hemispheric biomass burning season as recently published by Edwards et al. (2006). These CO enhancements have been attributed to forest fires in Africa and South America. The Michelson Interferometer for Passive Atmospheric Sounding (MIPAS) instrument provides a complementary dataset of this episode, namely upper tropospheric C_2H_6 and ozone volume mixing

ACPD

7, 12067–12095, 2007

ratios in October–November 2003. C_2H_6 is a direct biomass burning product generated predominantly by smouldering combustion (Lobert and Warnatz, 1993), while O_3 is generated from NO_x emissions by photochemistry. To our knowledge, our data are the first global upper tropospheric C_2H_6 data set which also covers tropical latitudes.

2 MIPAS Observations

MIPAS (Michelson Interferometer for Passive Atmospheric Sounding) is part of the instrumentation of the Environmental Satellite (ENVISAT) which was launched into its sun-synchronous polar orbit on 1 March 2002. It is a limb emission spectrometer designed primarily for measurement of stratospheric trace species from space (Fischer et al., 2007). Nevertheless, under cloud-free conditions it also provides information on upper tropospheric trace species. MIPAS was operational from July 2002 to March 2004 with full specification, in particular 0.05 cm^{-1} spectral resolution in terms of full width at half maximum (apodised with the "strong" Norton and Beer, 1976, function). Data presented here were recorded from 21 October to 14 November 2003, during Envisat orbits 8573 to 8931. The data analysis reported in this paper relies on the ESA-provided so-called level-1B data product version 4.59 which includes calibrated phase-corrected and geolocated radiance spectra (Nett et al., 1999). Spectra containing cloud signal were identified using a method suggested by Spang et al. (2004) and have been excluded from further analysis. The general strategy and formalism of the retrieval is discussed in detail in von Clarmann et al. (2003). In the following we restrict the discussion to specific issues of the retrieval of upper tropospheric C_2H_6 and ozone.

2.1 Ethane (C_2H_6)

Data presented in this paper are version V2_C2H6_1. Features in spectra of tangent altitudes of 33 km and lower have been analysed for C_2H_6. Its abundances are retrieved from the ν_9 fundamental emissions in the spectral region of 780–868 cm^{-1}. In

ACPD
7, 12067–12095, 2007

order to blank out regions with low C_2H_6 signal and large signal of other species, 30 so-called microwindows have been selected within the analysis window (Fig. 1). Interfering species in this spectral region are O_3, H_2O, HNO_3, $ClONO_2$, CFC-11, ClO, N_2O_5, HNO_4, CFC-12 and SF_6, for which pre-retrieved values were used, i.e. mixing ratios retrieved in a preceding analysis step from the same set of spectra but usually different microwindows. The interferents PAN and CCl_4 were considered on the basis of climatological profiles, which is justified because their radiance contribution within the microwindows chosen is low. A retrieved C_2H_6 profile has three to four degrees of freedom (i.e. independent pieces of information, calculated as the trace of the averaging kernel matrix, c.f. Rodgers, 2000), of which, at tropical geolocations where the tropopause is as high as 17 km, approximately three characterize the troposphere. Typical single profile total retrieval errors, i.e. noise and parameter errors excluding spectroscopic data uncertainties, for measurements of enhanced tropospheric C_2H_6 vary between about 20 and 50%, depending on altitude, temperature, humidity and actual C_2H_6 abundances. At all altitudes the error budget is dominated by measurement noise, which, from the lowest tangent altitude actually used up to 18 km, contributes an order of magnitude more than all other random error sources together. These other random errors we define are randomly varying errors due to uncertain instrumental or atmospheric parameters which might influence the retrieval, such as interfering species. The vertical resolution is about 3 to 4 km at 9 km altitude, as determined from the row of the averaging kernel matrix (Fig. 2). Above approximately 18–20 km, the C_2H_6 signal in the MIPAS spectra is so low that no more useful profile information can be retrieved.

A major issue with respect to the absolute accuracies of the retrieved C_2H_6 mixing ratios are spectroscopic data, which are currently under debate (personal communication J. Vander Auwera, 2005 and J.-M. Flaud, 2006). The line intensities in HITRAN2K (Rothman et al., 2003) which have been used for this analysis are a factor of 2 stronger than those in the GEISA spectroscopic database (Jacquinet-Husson et al., 2003), resulting in a factor of 2 lower mixing ratios. Line intensities of a more recent data set, which were not yet available at the time of this study, are about 30 percent smaller than

ACPD
7, 12067–12095, 2007

those used here (Vander Auwerra et al., 2007). These uncertainties, however, have no impact on our results since we analyse relative distributions only, which makes our analysis robust against any scalar bias, and results can easily be re-scaled for band-intensity correction, which is a commonly used approach in atmospheric spectroscopy.

Since the sensitivity of mid-infrared limb emission measurements to abundances of species in the troposphere is limited, data recorded between 21 October 2003 and 14 November 2003 were averaged in order to increase significance. In the following, we discuss the averaged spatial distributions of C_2H_6 in the upper troposphere, i.e. at 275 hPa, which corresponds roughly to 9–10 km altitude. At the given altitude resolution of the vertical profiles of 3 to 4 km, assessment of adjacent altitude levels does not provide much additional information.

Widespread high C_2H_6 were observed in the Northern hemisphere, which is attributed to industrial pollution (Fig. 3). Values of about 200–400 pptv were retrieved. The background mixing ratio in the Southern hemisphere was only about 75 pptv. However, there was a plume-like structure reaching from Brazil over the Southern tropical Atlantic Ocean, Southern Africa, the Southern subtropical Indian Ocean to Australia and beyond. Here values of 300–400 pptv were observed, which are comparable to those in polluted airmasses in the Northern hemisphere. The typical uncertainty of the mean mixing ratio in a longitude-latitude bin is about 30 pptv. Volume mixing ratios measured by MIPAS are approximately a factor of 2 lower than those measured by ACE during the biomass burning season 2004 (Rinsland et al., 2005), who used the 2976–2977 cm^{-1} spectral region. This discrepancy is most likely to be attributed to inconsistent spectroscopic data in these two bands. In situ measurements of about 500–700 pptv at 9 km altitude inside biomass burning plumes have been reported by Talbot et al. (1996). While the latter measurements were already taken in 1992, they also refer to a situation of enhanced vegetation fire activity.

ACPD
7, 12067–12095, 2007

2.2 O_3

The ozone distributions presented in this paper are version V2_O3_2, and their retrieval has been described in detail in Glatthor et al. (2006). The microwindows chosen are situated both in the MIPAS A band (685–970 cm^{-1}) and AB band (1020–1170 cm^{-1}) (Figs. 4 and 5). Detailed validation is presented by Steck et al. (2007b). Under tropical enhanced tropospheric ozone conditions, the retrieval has 2 to 3 degrees of freedom in the troposphere. Typical single profile retrieval errors are of the order of 50% or more for upper tropospheric background concentrations but are reduced to reasonable values by averaging over the observation period within latitude-longitude bins (see Sect. 2.1). At tropospheric altitudes the error budget is dominated by measurement noise, followed by uncertainties in spectral shift and temperature. The altitude resolution at 9 km altitude, as determined from the rows of the averaging kernel matrix (Fig. 2), is about 4 km. The standard error of the mean over the analysis period in a latitude-longitude bin of enhanced ozone is of the order of 3 ppbv.

O_3 abundances at 275 hPa are high towards polar latitudes where stratospheric air is seen (Fig. 6). Towards the tropics, values of only 0–50 ppbv were observed both in northern and southern low latitudes. Only in parts of the plume-like region of polluted air described above where enhanced C_2H_6 was observed, O_3 mixing ratios of up to 80 ppbv are observed.

2.3 CFC-11

In this study the volume mixing ratio of CFC-11 is used as an indicator to distinguish between tropospheric and stratospheric air. CFC-11 is retrieved in the 838.0–853.0 cm^{-1} spectral region, which covers the ν_4 band (Fig. 7). Main interfering lines in this region are associated to H_2O, HNO_3 and $COCl_2$. In order to avoid propagation of uncertainties of a priori knowledge on these species to the CFC-11 profiles, their abundances are joint-fitted in the CFC-11-analysis window. The estimated total retrieval error of tropospheric CFC-11 is only 4–9% except for particularly moist atmospheric conditions

where enhanced opacity of the atmosphere due to water vapour emissions or even undetected thin clouds affect the retrieval. Besides this, the main component of the CFC-11 retrieval error is line-of-sight uncertainties, which even outweigh the contribution of measurement noise. The altitude resolution is about 3.3 km. The tropical troposphere is characterized by three to four degrees of freedom of the retrieved CFC-11 profile. A dedicated paper on the retrieval of CFC-11 from MIPAS spectra and validation is in preparation. A global map of CFC-11 at 275 hPa is shown in Fig. 8. The standard error of the mean value within a latitude-longitude bin typically is around 5 pptv.

3 Southern hemispheric pollution belt

As we will discuss in the following, the enhanced Southern hemispheric mixing ratios of tropospheric C_2H_6 and O_3 are attributed to biomass burning in South America, Africa, Australia and Indonesia. For a similar period, MOPITT measured enhanced CO, which has also been attributed to biomass burning. The CO plume presented by Edwards et al. (2006) (their Fig. 1b) coincides nicely with the region of enhanced C_2H_6, PAN (Glatthor et al., 2007), and O_3 detected by MIPAS.

3.1 Trajectory calculations

In order to assign the detected plume-like belt of polluted air to biomass burning, 12-day forward trajectories have been calculated with the HYSPLIT model (Draxler and Hess, 1997, 1998) (see also: http://www.arl.noaa.gov/ready/hysplit4.html), based on European Centre for Midrange Weather Forecast (ECMWF) analysis data. The trajectories were started at 4500 m altitude for Southern African fires and at 2500 m altitude for South American, Indonesian and Australian fires. These trajectory altitudes comply with the so-called "injection altitude", i.e. upper boundary of the mixing layer, which was found typical for biomass fires in these regions by Labonne et al. (2007). However, it should be mentioned that the final trajectory pattern varies only marginally with the in-

ACPD
7, 12067–12095, 2007

jection altitude varying between 2500 and 4500 m. Burning areas were identified using daily Tropical Rainfall Measuring Mission (TRMM) Visible and Infrared Scanner (VIRS) satellite data (Giglio et al., 2000). As starting points of plume trajectories locations were selected where clusters of TRMM fire counts were found in the time interval 9 October 2003 to 14 November 2003, i.e., in the observation period of which data are presented here plus an 12-day extension towards earlier days to allow aged plume air to be detected. One trajectory represents approximately 10 fire counts. Results of the trajectory calculations are shown in Fig. 9.

3.2 Plume tracer C_2H_6

The bulk of biomass burning plume trajectories, in particular those starting from tropical America and Africa, covers the same geolocations where enhanced C_2H_6 is seen. C_2H_6, like other non-methane hydrocarbons, is generated by both flaming and smouldering combustion (Lobert and Warnatz, 1993) but larger quantities are produced via smouldering combustion (Crutzen and Andreae, 1990). Its expected atmospheric lifetime in the upper troposphere is estimated at 100 days (Mauzerall et al., 1998), which is much longer than the episode under analysis. This suggests that, among the available MIPAS data, C_2H_6 is a suitable tracer for plumes of polluted air. In order to define a threshold for plume air, the average value and the standard deviation of the C_2H_6 mixing ratios of all tropical and Southern hemispheric (i.e. 15° N to 90° S) 5°×15° latitude-longitude bins not touched by any of the trajectories was calculated. The average (weighted by the inverse variance of the mean value of each bin) is 66 pptv and is understood to represent the Southern hemispheric background mixing ratio at 275 hPa. The average plus two standard deviations is 180 pptv and is considered a suitable threshold for plume air (Fig. 10). This threshold reduces the one-sided risk that background air is misinterpreted as plume air, but does not minimize the complementary risk, i.e., plume air parcels may remain undetected, in particular in the Pacific area, where presumably more divergent trajectories lead to smaller C_2H_6 mixing ratios.

3.3 Ozone morphology within the plume

Ozone is an indirect biomass burning product. It is generated photochemically from excess NO_2 which is a primary biomass burning product. MIPAS ozone observations vary considerably within the biomass burning plume. In particular, the part of the plume attributed to African savanna fires contains much more ozone compared to the equatorial American rain forest fire plume (Fig. 11). The mean O_3/C_2H_6 ratio is 242 in the African plume but only 210 in the Amazonian plume. In the Australian part of the plume high ozone values (above 100 ppbv) are observed, too, but these are attributed to stratospheric signal, as discussed below in Sect. 3.4.

3.4 Removal of stratospheric signal

High ozone mixing ratios along with low C_2H_6 values in the Australian part of the plume suggest that the ozone seen at 275 hPa might be affected by a stratospheric ozone signal. The ozone signal at this altitude can be contaminated by stratospheric ozone by two mechanisms of entirely different nature: Either stratospheric air could have been mixed or transported into the upper troposphere; or, in the case of a low tropopause, due to the limited altitude resolution of the MIPAS ozone retrievals, stratospheric ozone could be misinterpreted as upper tropospheric ozone. In the given context, however, it is not necessary to distinguish between both these causes of stratospheric signal, since the effect would be the same: Stratospheric ozone would erroneously be attributed to a biomass burning plume. To determine data bins which are dominated by any of these potentially stratospheric ozone signals mentioned above, we use CFC-11 as a tracer. CFC-11 is a tropospheric species with mixing ratios rapidly decreasing with altitude in the stratosphere. Further, CFC-11 is long-lived and well-mixed in the troposphere and its mixing ratios are not driven by fire events. Its averaging kernels in the tropopause region are of similar width as those of ozone. Therefore, low CFC-11 values hint at a stratospheric ozone signal in the observed data bin.

Indeed some plume bins related to trajectories starting in Australia are character-

ACPD
7, 12067–12095, 2007

EGU

ized by low CFC-11 mixing ratios. This applies to data bins over the Pacific Ocean and the Southern Atlantic east of Southern Argentina and explains the high O_3/C_2H_6 ratios (green symbols in Fig. 11). Air parcels with CFC-11 mixing ratios below 245 pptv were rejected from further analysis. This particular threshold removed most of the spurious data points with high ozone and low C_2H_6 mixing ratios which are attributed to stratospheric contamination. On the other hand, this threshold left enough data points for statistical analysis. Indeed the right panel of Fig. 11, which shows O_3 mixing ratio over C_2H_6 after application of the CFC-11 filter, includes much less data points with high (possibly stratospheric) ozone and low C_2H_6 compared to the unfiltered scatter plot. Nevertheless, some suspicious data points with high O_3 and low C_2H_6 remain even after application of the CFC-11 filter, which presumably is not sensitive enough to remove all stratospheric ozone signal. This sub-optimal behaviour of the CFC-11 filter is attributed to its application on bin averages without consideration of the typically nonlinear correlation of O_3 and CFC-11. Therefore, we restrict the further investigation of plume ozone to the South American and African plumes. The contrast between the O_3/C_2H_6 ratios of the Amazonian and African plumes is enhanced through this data filter: After application of the filter the ratios are 230 for the African plume and 185 for the Amazonian one.

3.5 Discussion

Tropical rain forest fire emissions mostly occur near the inner tropic convergence zone and it is obvious that emitted gases can be rapidly transported to the altitudes of interest (i.e. seen by MIPAS) by convection (Greco et al., 1990; Andreae et al., 2001). For subtropical savanna fire emissions, the situation is not that clear because of predominant subsidence of air masses at these latitudes. Certainly, fires provide additional heating at the surface which attributes to convection. Nevertheless, during convection colder ambient air is always mixed into the air parcel to be lifted and it is not quite clear, which altitudes can be reached. Chatfield et al. (2002), however, report frequent final pollutant injection by cloud convection over Southern Africa in September–October

1997. These authors mention both thunderstorm-scale venting as well as synoptic scale venting as mechanisms of uplifting of pyrogenic pollution. However, no pyrogenic deep convection has to our knowledge been reported for subtropical conditions with prevailing subsidence. Trentmann et al. (2006) state that the nature of pyro-convection is not fully understood, and Luderer et al. (2006) have shown that pyro-convection depends largely on the actual background meteorology. Another mechanism of uplifting pyrogenic pollution under the subsiding branch of the Hadley cell into the upper troposphere has been proposed by Andreae et al. (2001): The polluted air is transported into the tropics at lower levels and lofted there by deep convection. Typical uplifting mechanisms for African biomass burning plume air are discussed in Chatfield et al. (1998). The area where pyro-polluted air reaches higher altitudes was identified to be the Congo basin (c.f. Figs 5 e and f in their paper). In our study, we try to appropriately characterize the uplifting and transport process by starting the trajectory calculations at the so-called "injection altitude", an altitude empirically determined by Labonne et al. (2007) and found consistent with the upper edge of the boundary layer. Tests have shown that the final trajectory pattern is quite robust against variation of the assumed injection altitude in a range from 2500 to 4500 m. Certainly, our approach misses any subsynoptic uplifting taking place above the mixing layer.

Different plume composition may be caused by different type of vegetation burning, different combustion stage, the actual meteorological conditions including illumination and uplifting mechanisms, aging in different chemical environments, mixing etc. One possible explanation for the lower O_3/C_2H_6 ratio in the Amazonian plume is that rainforest fires with predominantly smouldering combustion emit more C_2H_6 than African biomass burning, where flaming grassland and savanna fires are prevailing (Delmas et al., 1999). Relatively low ozone in the Amazonian plume was also found by Bremer et al. (2004). These authors attribute it to significant photochemical evolution involving strong reduction of NO_x lifetime related to oxygenated volatile organic compound chemistry.

Different residence time of pyro-polluted air in the lower troposphere with different

prevailing chemistry is, beyond different pollutant source strengths of savanna versus rainforest and smouldering versus flaming combustion, a further candidate explanation of different mean O_3/C_2H_6 ratios. This would suggest that African savanna-fire pyro-polluted air resides longer in the lower troposphere compared to its Amazonian counterpart. Furthermore, additional upper tropospheric ozone can also be produced by lightning-induced NO_2 and thus depends on thunderstorm activity along the actual trajectories (Staudt et al., 2002; Edwards et al., 2003). No evidence for a relation between the mean age of the trajectories falling within a bin and the O_3 enhancement has been found. The large variability of O_3/C_2H_6 ratios and low correlation coefficients inside the belt of polluted air ($-0.06<r<0.06$ for all cases analysed, i.e. Amazonian and African plume, with and without CFC-11 filter) reflect how important the individual chemical history of each air parcel is for the efficiency of upper tropospheric ozone production within the biomass burning plumes. Of course, the fact that O_3 and C_2H_6 mixing ratios are uncorrelated within the belt of polluted air does not affect our finding that enhanced ozone mixing ratios at low latitudes are confined to the belt of polluted air where also C_2H_6 mixing ratios are enhanced.

4 Conclusions

Southern hemispheric C_2H_6 generated by biomass burning reaches similar abundances as Northern hemispheric enhancements. The MIPAS measurements of Southern hemispheric C_2H_6 nicely confirm the spatial extension of the biomass burning plume reported by Edwards et al. (2006) and complement the dataset published by these authors. African and South American forest fires appear to be the major source of Southern hemispheric upper tropospheric C_2H_6 during the episode under analysis, since enhanced mixing ratios are confined to regions covered by trajectories started above fire events. However, a signal of other anthropogenic pollution sources, e.g. from megacities or industrial plants (Talbot et al., 1996) in the vicinity of forest fires cannot be excluded. At least at tropical latitudes where the possibility of con-

tamination of the measured signal by a stratospheric contribution can safely be excluded, upper tropospheric ozone enhancements are confined to the pollution belt. Flaming combustion, which is prevailing in Southern African fires, is seen on a hemispheric scale to contribute more efficiently to a high upper tropospheric O_3/C_2H_6 ratio than smouldering combustion which is typical for the Amazonian rain forest. The final decision on whether the observed differences in ozone production are primarily driven by different trace gas loading in the plume through different types of combustion, or whether they are driven by different prevailing uplifting processes keeping the air in different chemical regimes remains speculative without the explicit consideration of small-scale convective processes in the trajectory calculation. Further studies on this and related questions will benefit from MIPAS measurements of further biomass burning related species, particularly CO[1], PAN and C_2H_2 (Glatthor et al., 2007), and H_2CO (Steck et al., 2007a), which confirm the extension of the plume-like pollution belt in the Southern hemisphere of 2003. Further, the analysis of data recorded before and after the biomass burning season is planned in order to detect other sources of these pollutants, e.g. megacities and industrial plants. A possible improvement of the absolute accuracy of our C_2H_6 retrievals by use of the most recent spectroscopic data will be investigated. The data of this study are available to registered users via http://www.fzk.de/imk/asf/ame/envisat-data/.

Acknowledgements. ESA has provided MIPAS Level-1B data. Meteorological analysis data used for retrieval calculations were provided by ECMWF. A. Linden and T. Steck have been funded by Helmholtz Gemeinschaft Deutscher Großforschungszentren under Virtual Institute IMACCO, contract number VH-VI-117. S. Kellmann has been funded by BMBF under contract number 50 EE 0512.

[1]B. Funke et al.: article in preparation, 2007.

References

Andreae, M. O., Artaxo, P., Fischer, H., Freitas, S. R., Grégoire, J.-M., Hansel, A., Hoor, P., Kormann, R., Krejci, R., Lange, L., Lelieveld, J., Lindinger, W., Longo, K., Peters, W., de Reus, M., Scheeren, B., Silva Dias, M. A. F., Ström, J., van Velthoven, P. F. J., and Williams, J.: Transport of biomass burning smoke to the upper troposphere by deep convection in the equatorial region, Geophys. Res. Lett., 28, 951–954, 2001. 12076, 12077

Bremer, H., Kar, J., Drummond, J. R., Nichitu, F., Zou, J., Liu, J., Gille, J. C., Deeter, M. N., Francis, G., Ziskin, D., and Warner, J.: Spatial and temporal variation of MOPITT CO in Africa and South America: A comparison with SHADOZ ozone and MODIS aerosol, J. Geophys. Res., 109, doi:10.1029/2003JD004234, 2004. 12077

Chatfield, R. B., Vastano, J. A., Li, L., Sachse, G. W., and Connors, V. S.: The Great African plume from biomass burning: Generalizations from a three-dimensional study of TRACE A carbon monoxide, J. Geophys. Res., 103, 28 059–28 077, 1998. 12077

Chatfield, R. B., Guo, Z., Sachse, G. W., Blake, D. R., and Blake, N. J.: The subtropical global plume in the Pacific Exploratory Mission-Tropics A (PEM-Tropics A), PEM-Tropics B, and the Global Atmospheric Sampling Program (GASP: How tropical emissions affest the remote Pacific, J. Geophys. Res., 4278, doi:10.1029/2001/JD000497, 2002. 12076

Coheur, P., Herbin, H., Clerbaux, C., Hurtmans, D., Wespes, C., Carleer, M., Turquety, S., Rinsland, C. P., Remedios, J., Hauglustaine, D., Boone, C. D., and Bernath, P. F.: ACE-FTS observation of a young biomass burning plume: first reported measurements of C_2H_4, C_3H_6O, H_2CO and PAN by infrared occultation from space, Atmos. Chem. Phys. Discuss., 7, 7907–7932, 2007, http://www.atmos-chem-phys-discuss.net/7/7907/2007/. 12068

Crutzen, P. J. and Andreae, M. O.: Biomass Burning in the Tropics: Impact on Atmospheric Chemistry and Biogeochemical Cycles, Science, 250, 1669–1678, 1990. 12074

Delmas, R. A., Druilhet, A., Cros, B., Durand, P., Delon, C., Lacaux, J. P., Brustet, J. M., Serca, D., Affre, C., Guenther, A., Greenberg, J., Baugh, W., Harley, P., Klinger, L., Brasseur, P. G. G., Zimmerman, P. R., Grégoire, J. M., Janodet, E., Tournier, A., Perros, P., Marion, T., Gaudichet, A., Ruellan, H. C. S., Cautenet, P. M. S., Bouka Biona, D. P. C., Nganga, D., Tathy, J. P., Minga, A., Loemba–Ndembi, J., and Ceccato, P.: Experiment for Regional Sources and Sinks of Oxidants (EXPRESSO): An overview, J. Geophys. Res., 104, 30 609–30 624, 1999. 12077

Draxler, R. R. and Hess, G. D.: Description of the HYSPLIT_4 modeling system, nOAA Tech. Memo. ERL ARL-224, 24pp., 1997. 12073

Draxler, R. R. and Hess, G. D.: An overview of the HYSPLIT_4 modelling system for trajectories, dispersion and deposition, Australian Meteorological Magazine, 47, 295–308, 1998. 12073

Edwards, D. P., Lamarque, J.-F., Attié, J.-L., Emmons, L. K., Richter, A., Cammas, J.-P., Gille, J. C., Francis, G. L., Deeter, M. N., Warner, J., Ziskin, D. C., Lyjak, L. V., Drummond, J. R., and Burrows, J. P.: Tropospheric ozone over the tropical Atlantic: A satellite perspective, J. Geophys. Res., 108, 4237, doi:10.1029/2002JD002927, 2003. 12078

Edwards, D. P., Emmons, L. K., Gille, J. C., Chu, A., Attié, J.-L., Giglio, L., Wood, S. W., Haywood, J., Deeter, M. N., Massie, S. T., Ziskin, D. C., and Drummond, J. R.: Satellite-observed pollution from Southern Hemisphere biomass burning, J. Geophys. Res., 111, D14312, doi:10.1029/2005JD006655, 2006. 12068, 12073, 12078

Fischer, H., Birk, M., Blom, C., Carli, B., Carlotti, M., von Clarmann, T., Delbouille, L., Dudhia, A., Ehhalt, D., Endemann, M., Flaud, J. M., Gessner, R., Kleinert, A., Koopmann, R., Langen, J., López-Puertas, M., Mosner, P., Nett, H., Oelhaf, H., Perron, G., Remedios, J., Ridolfi, M., Stiller, G., and Zander, R.: MIPAS: an instrument for atmospheric and climate research, Atmos. Chem. Phys. Discuss., 7, 8795–8893, 2007, http://www.atmos-chem-phys-discuss.net/7/8795/2007/. 12069

Giglio, L., Kendall, J. D., and Tucker, C. J.: Remote sensing of fires with the TRMM VIRS, Int. J. Remote Sensing, 21, 203–207, 2000. 12074

Glatthor, N., von Clarmann, T., Fischer, H., Funke, B., Gil-López, S., Grabowski, U., Höpfner, M., Kellmann, S., Linden, A., López-Puertas, M., Mengistu Tsidu, G., Milz, M., Steck, T., Stiller, G. P., and Wang, D.-Y.: Retrieval of stratospheric ozone profiles from MIPAS/ENVISAT limb emission spectra: a sensitivity study, Atmos. Chem. Phys., 6, 2767–2781, 2006, http://www.atmos-chem-phys.net/6/2767/2006/. 12072

Glatthor, N., von Clarmann, T., Fischer, H., Funke, B., Grabowski, U., Höpfner, M., Kellmann, S., Kiefer, M., Linden, A., Milz, M., Steck, T., and Stiller, G. P.: Global peroxyacetyl nitrate (PAN) retrieval in the upper troposphere from limb emission spectra of the Michelson Interferometer for Passive Atmospheric Sounding (MIPAS), Atmos. Chem. Phys., 7, 2775–2787, 2007, http://www.atmos-chem-phys.net/7/2775/2007/. 12073, 12079

Greco, S., Swap, R., Garstang, M., Ulanski, S., Shipman, M., Harriss, R. C., Talbot, R., Andreae, M. O., and Artaxo, P.: Rainfall and surface kinematic condition over central Amazonia during ABLE-2A, J. Geophys. Res., 95, 17 001–17 014, 1990. 12076

Jacquinet-Husson, N., Scott, N. A., Chédin, A., and Chursin, A. A.: The GEISA spectroscopic database system updated for IASI (direct radiative transfer modeling), Atmos. Oceanic Opt., 16, 256–261, 2003. 12070

Labonne, M., Bréon, F., and Chevallier, F.: Injection height of biomass burning aerosols as seen from a spaceborne lidar, Geophys. Res. Lett., 34, L11 806, doi:10.1019/2007GL029311, 2007. 12073, 12077

Lobert, J. M. and Warnatz, J.: Emissions from the Combustion Process in Vegetation, in: Fire in the Environment: The Ecological, Atmospheric, and Climatic Importance of Vegetation Fires, edited by: Crutzen, P. J. and Goldammer, J. G., pp. 15–51, John Wiley & Sons Ltd, 1993. 12069, 12074

Luderer, G., Trentmann, J., Winterrath, T., Textor, C., Herzog, M., Graf, H. F., and Andreae, M. O.: Modeling of biomass smoke injection into the lower stratosphere by a large forest fire (Part II): sensitivity studies, Atmos. Chem. Phys., 6, 5261–5277, 2006, http://www.atmos-chem-phys.net/6/5261/2006/. 12077

Mauzerall, D. L., Logan, J. A., Jacob, D. J., Anderson, B. E., Blake, D. R., Bradshaw, J. D., Heikes, B., Sachse, G. W., Singh, H., and Talbot, B.: Photochemistry in biomass burning plumes and implications for tropospheric ozone over the tropical South Atlantic, J. Geophys. Res., 103, 8401–8423, 1998. 12074

Nett, H., Carli, B., Carlotti, M., Dudhia, A., Fischer, H., Flaud, J.-M., Perron, G., Raspollini, P., and Ridolfi, M.: MIPAS Ground Processor and Data Products, in: Proc. IEEE 1999 International Geoscience and Remote Sensing Symposium, 28 June–2 July 1999, Hamburg, Germany, pp. 1692–1696, 1999. 12069

Norton, H. and Beer, R.: New apodizing functions for Fourier spectrometry, J. Opt. Soc. Am, 66, 259–264, (Errata J. Opt. Soc. Am., 67, 419, 1977), 1976. 12069

Rinsland, C. P., Dufour, G., Boone, C., Bernath, P., and Chiou, L.: Atmospheric Chemistry Experiment (ACE) measurements of elevated Southern Hemisphere upper tropospheric CO, C_2H_6, HCN, and C_2H_2 mixing ratios from biomass burning emissions and long-range transport, Geophys. Res. Lett., 32, L20803, doi:10.1029/2005GL024214, 2005. 12068, 12071

Rodgers, C. D.: Inverse Methods for Atmospheric Sounding: Theory and Practice, in: Series on Atmospheric, Oceanic and Planetary Physics, vol. 2, edited by: F. W. Taylor, World Scientific, 2000. 12070

Rothman, L. S., Barbe, A., Benner, D. C., Brown, L. R., Camy-Peyret, C., Carleer, M. R., Chance, K., Clerbaux, C., Dana, V., Devi, V. M., Fayt, A., Flaud, J.-M., Gamche, R. R.,

Goldman, A., Jacquemart, D., Jucks, K. W., Lafferty, W. J., Mandin, J.-Y., Massie, S. T., Nemtchinov, V., Newnham, D. A., Perrin, A., Rinsland, C. P., Schroeder, J., Smith, K. M., Smith, M. A. H., Tang, K., Toth, R. A., Vander Auwera, J., Varanasi, P., and Yoshino, K.: The HITRAN molecular spectroscopic database: edition of 2000 including updates through 2001, J. Quant. Spectrosc. Ra., 82, 5–44, doi:10.1016/S0022-4073(03)00146-8, 2003. 12070

Spang, R., Remedios, J. J., and Barkley, M. P.: Colour indices for the detection and differentiation of cloud types in infra-red limb emission spectra, Adv. Space Res., 33, 1041–1047, 2004. 12069

Staudt, A. C., Jacob, D. J., Logan, J. A., Bacchiochi, D., Krishnamurti, T. N., and Poisson, N.: Global chemical model analysis of biomass burning and lightning influences over the South Pacific in austral spring, J. Geophys. Res., 107, doi:10.1029/2000JD00296, 2002. 12078

Steck, T., Glatthor, N., von Clarmann, T., Grabowski, U., Höpfner, M., Kellmann, S., Kiefer, M., Linden, A., Milz, M., Stiller, G. P., Fischer, H., Funke, B., Perrin, A., and Flaud, J.: Retrieval of formaldehyde from high-resolution MIPAS-Envisat spectra, eNVISAT Symposium 2007, Montreux, Switzerland, 23–27 April, 2007a. 12079

Steck, T., von Clarmann, T., Fischer, H., Funke, B., Glatthor, N., Grabowski, U., Höpfner, M., Kellmann, S., Kiefer, M., Linden, A., Milz, M., Stiller, G. P., Wang, D. Y., Allaart, M., Blumenstock, T., von der Gathen, P., Hansen, G., Hase, F., Hochschild, G., Kopp, G., Kyrö, E., Oelhaf, H., Raffalski, U., Redondas Marrero, A., Remsberg, E., Russell III, J., Stebel, K., Steinbrecht, W., Wetzel, G., Yela, M., and Zhang, G.: Bias determination and precision validation of ozone profiles from MIPAS-Envisat retrieved with the IMK-IAA processor, Atmos. Chem. Phys., 7, 3639–3662, 2007, http://www.atmos-chem-phys.net/7/3639/2007/. 12072

Talbot, R. W., Bradshaw, J. D., Sandholm, S. T., Smyth, S., Blake, D. R., Blake, N. R., Sachse, G. W., Collins, J. E., Heikes, B. G., Anderson, B. E., Gregory, G. L., Singh, H. B., Lefer, B. L., and Bachmeier, A. S.: Chemical characteristics of continental outflow over the tropical South Atlantic Ocean from Brazil and Africa, J. Geophys. Res., 101, 24 187–24 202, 1996. 12071, 12078

Trentmann, J., Luderer, G., Winterrath, T., Fromm, M. D., Textor, C., Herzog, M., Graf, H. F., and Andreae, M. O.: Modeling of biomass smoke injection into the lower stratosphere by a large forest fire (Part I): reference simulation, Atmos. Chem. Phys., 6, 5247–5260, 2006, http://www.atmos-chem-phys.net/6/5247/2006/. 12077

Vander Auwerra, J., Moazzen-Ahmadi, N., and Flaud, J.: Toward an accurate database for

the 12 μm region of the ethane spectrum, The Astrophysical Journal, 662, 750–757, 2007. 12071

von Clarmann, T., Glatthor, N., Grabowski, U., Höpfner, M., Kellmann, S., Kiefer, M., Linden, A., Mengistu Tsidu, G., Milz, M., Steck, T., Stiller, G. P., Wang, D. Y., Fischer, H., Funke, B., Gil-López, S., and López-Puertas, M.: Retrieval of temperature and tangent altitude pointing from limb emission spectra recorded from space by the Michelson Interferometer for Passive Atmospheric Sounding (MIPAS), J. Geophys. Res., 108, 4736, doi:10.1029/2003JD003602, 2003. 12069

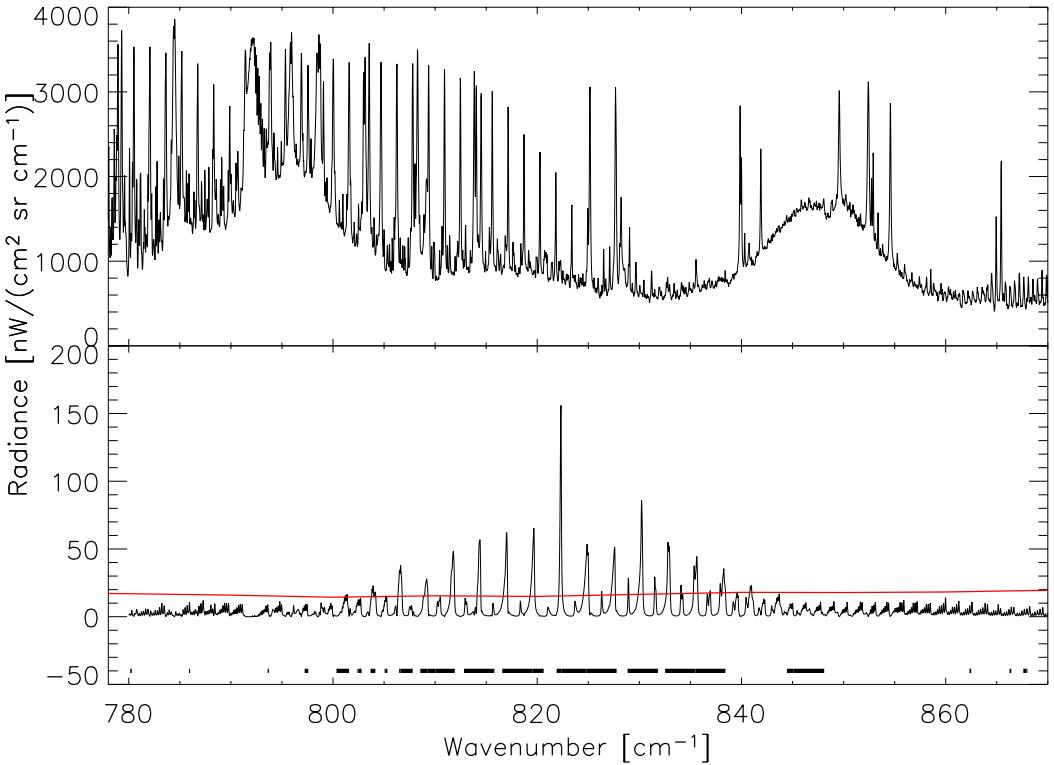

Fig. 1. MIPAS spectrum in the wavenumber range where C_2H_6 is analysed, measured at 13.0° S, 37.2° E on 21 October 2003, 10.06 km tangent altitude (upper panel). The lower panel is the C_2H_6 signal, determined by subtracting a calculated spectrum with zero C_2H_6 in the target altitude region (8–12 km) from the best fitting calculated spectrum. Microwindows are indicated as horizontal bars. The horizontal red line is the noise equivalent spectral radiance.

ACPD
7, 12067–12095, 2007

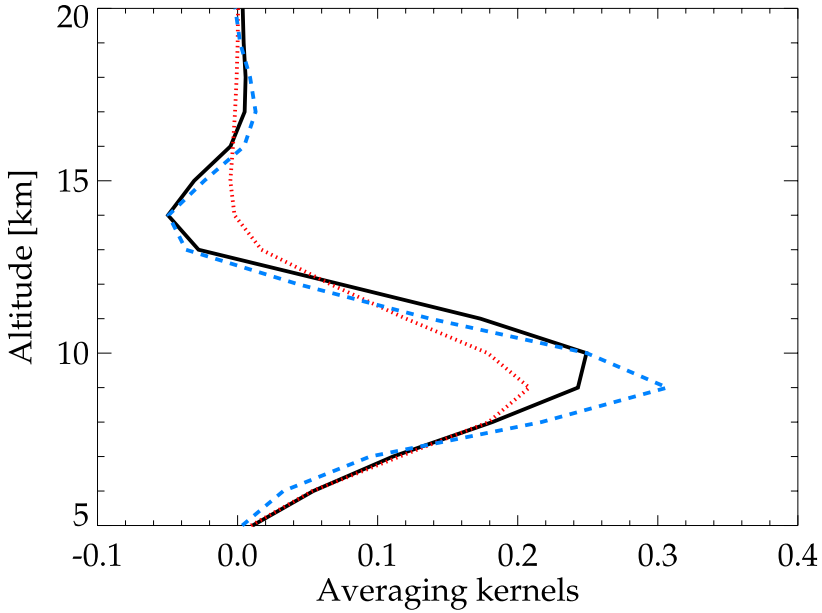

Fig. 2. Rows of averaging kernels at 9 km altitude for C_2H_6 (black, solid), O_3 (red, dotted), and CFC-11 (blue, dashed) for a profile measured on 21 October 2003 at 13.0° S, 37.2° E.

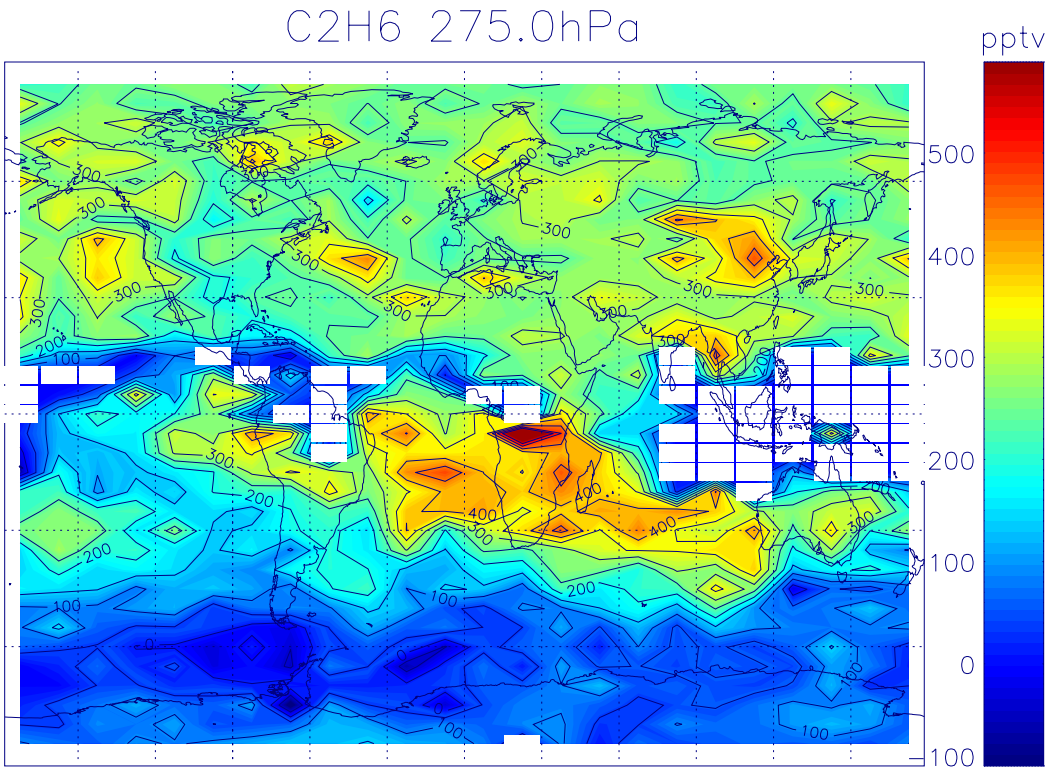

Fig. 3. VMR distribution of C_2H_6 at 275 hPa, averaged from 21 October to 14 November 2003. Larger mixing ratios are found in the Northern hemisphere, due to industrial pollution. In the Southern hemisphere a plume-like structure is visible.

ACPD
7, 12067–12095, 2007

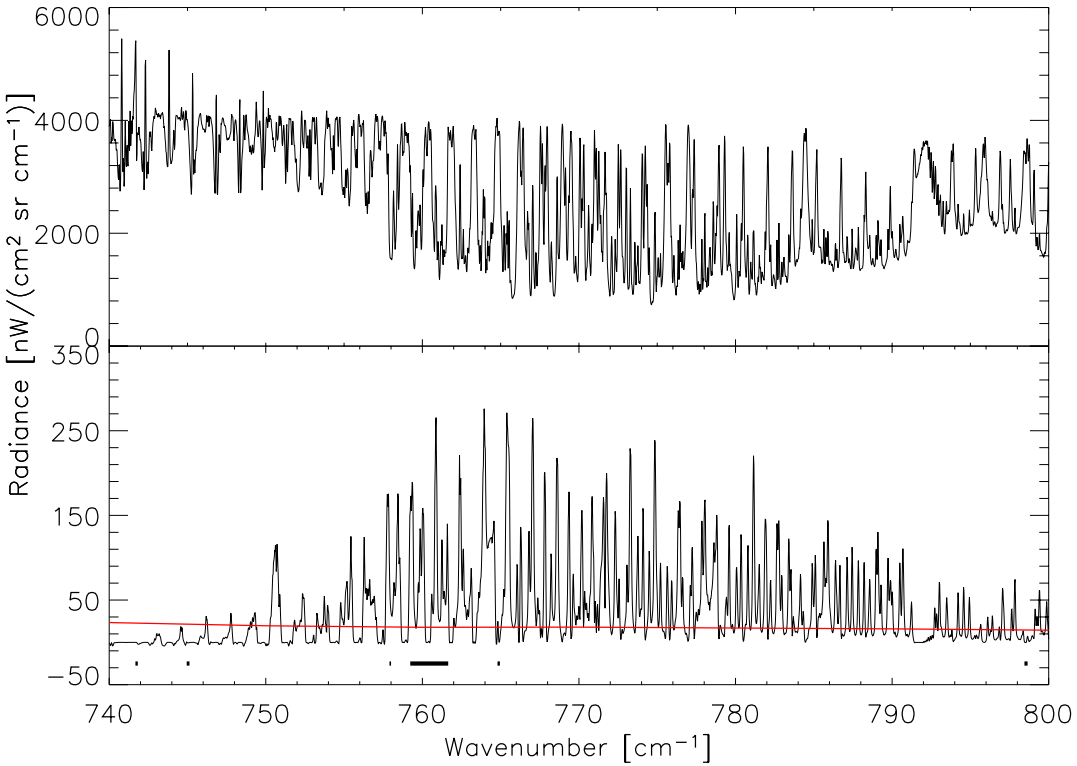

Fig. 4. MIPAS A band spectrum in the wavenumber range where O_3 is analysed. See Fig. 1 for details.

ACPD

7, 12067–12095, 2007

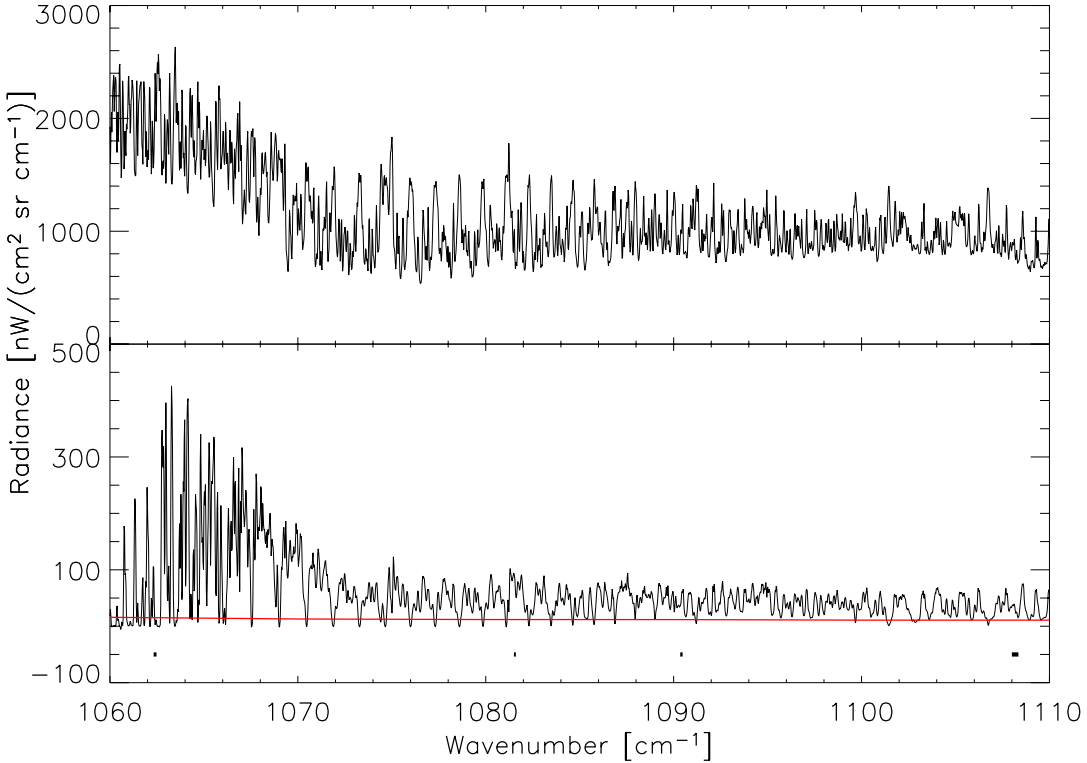

Fig. 5. MIPAS AB band spectrum in the wavenumber range where O_3 is analysed. See Fig. 1 for details.

ACPD

7, 12067–12095, 2007

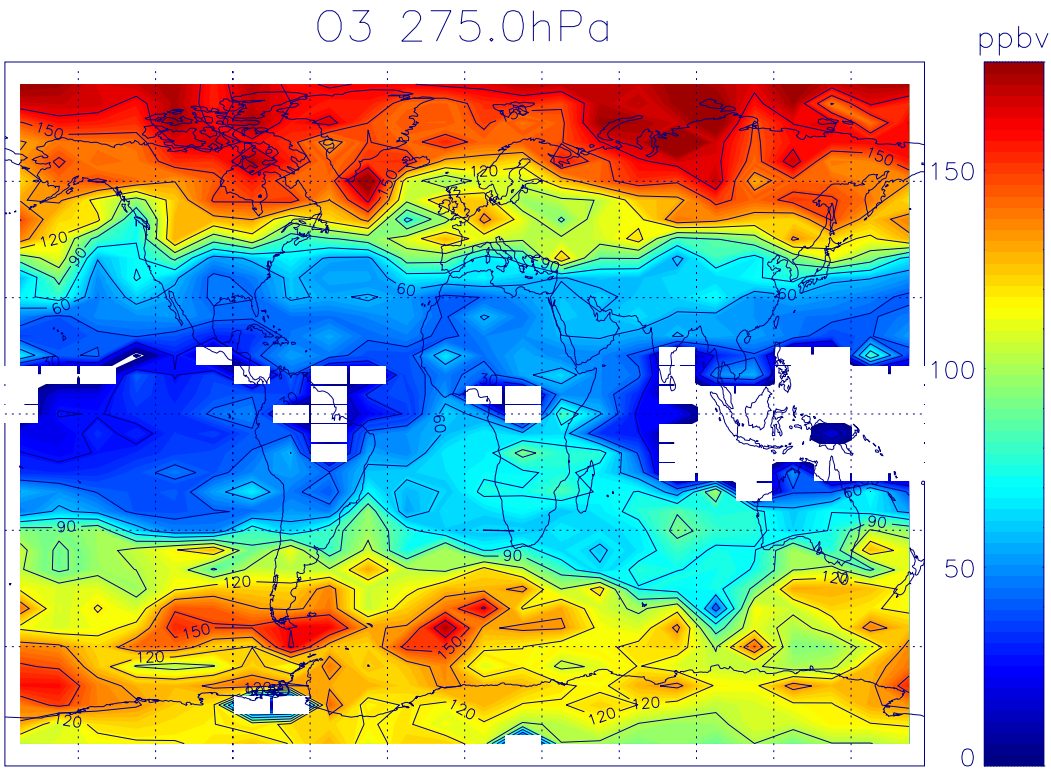

Fig. 6. VMR distribution of O_3 at 275 hPa, averaged from 21 October to 14 November 2003. Larger mixing ratios are found at northern and southern latitudes, where stratospheric air is sounded at this altitude. Enhanced tropospheric ozone is observed within the plume.

ACPD
7, 12067–12095, 2007

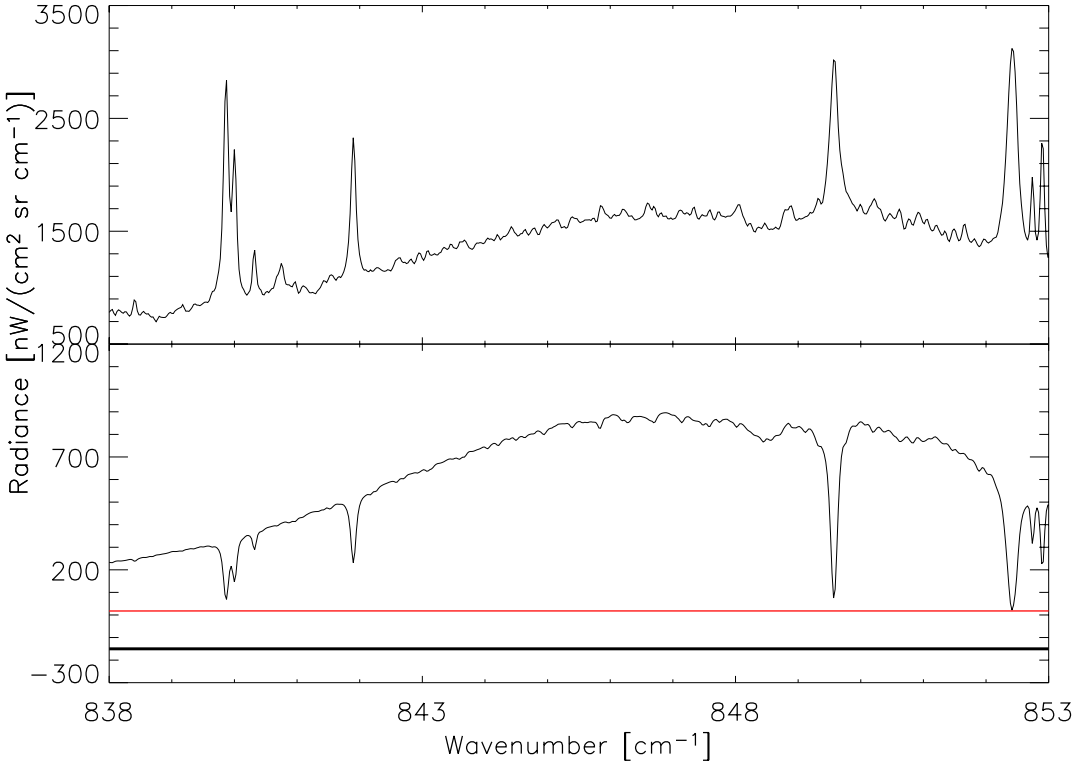

Fig. 7. MIPAS spectrum in the wavenumber range where CFC-11 is analysed. See Fig. 1 for details.

ACPD

7, 12067–12095, 2007

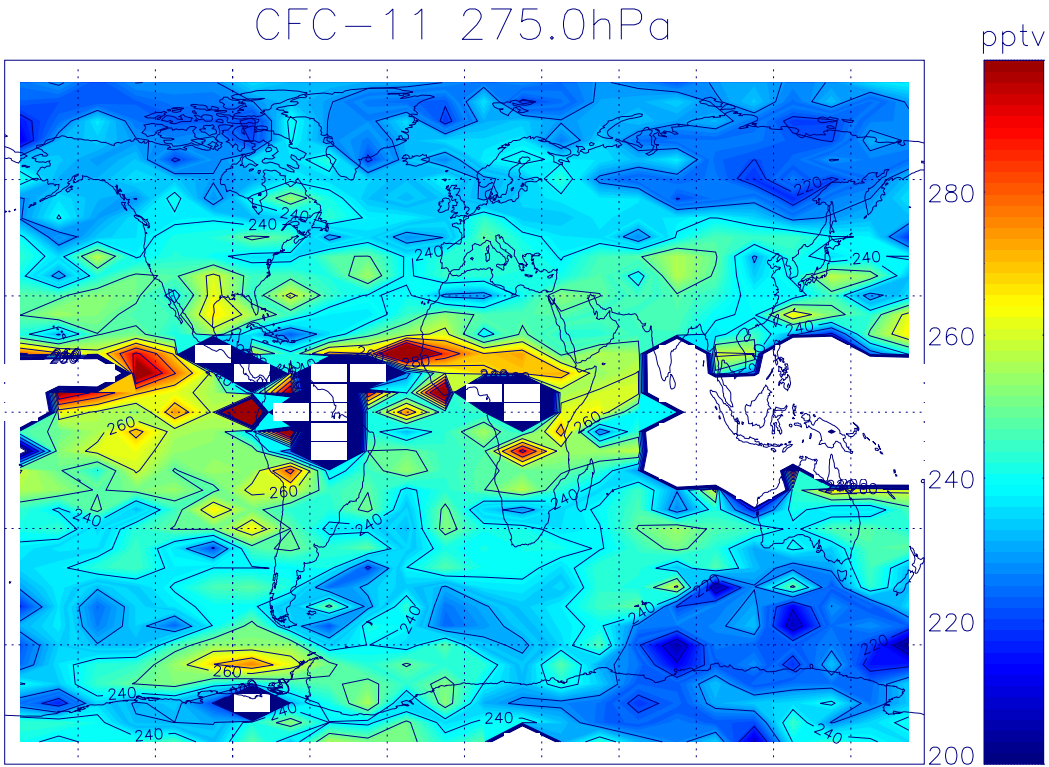

Fig. 8. VMR distribution of CFC-11 at 275 hPa, averaged from 21 October to 14 November 2003. Low values at high latitudes indicate stratospheric air sounded by MIPAS. Particularly high values near the equator most probably are artefacts due to extreme moisture or even undetected cloud signal in the spectra, to which the CFC-11 retrieval proves to be particularly sensitive.

ACPD
7, 12067–12095, 2007

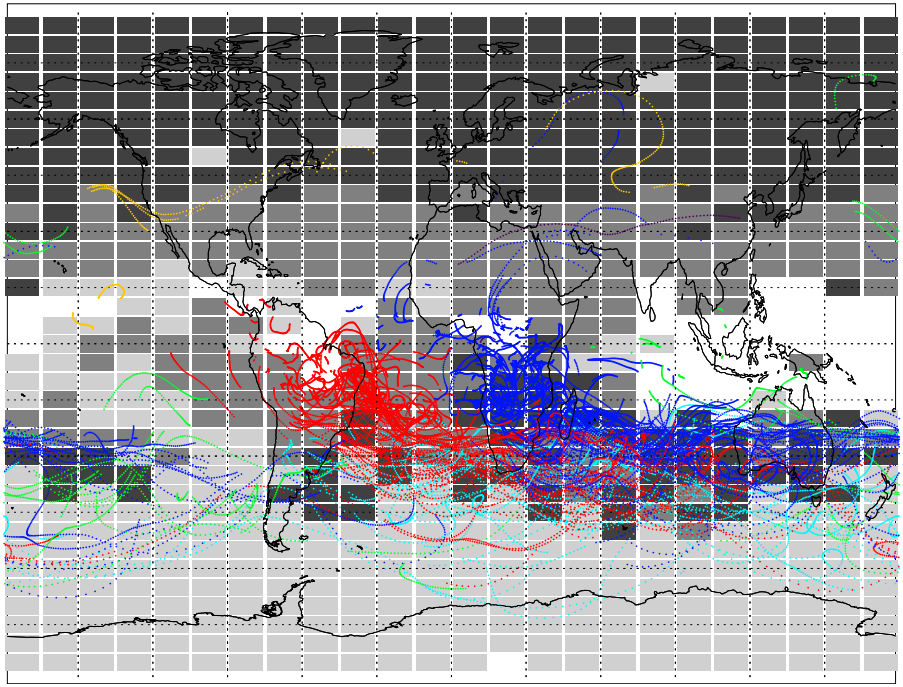

Fig. 9. Trajectories starting at geolocations of fire count clusters in the period from 13 October to 14 November 2003. Colour coding reflects the different starting points: blue = Africa, red = tropical America, yellow = North America, light blue = southernmost America, green = Australia and Indonesia. Only those points of the trajectories are shown which fall between 7 and 11 km, i.e. the measurement altitude plus/minus approximately half an altitude resolution of the MIPAS measurement. White background shading indicates data gaps due to clouds within the MIPAS field of view. Light grey corresponds to C_2H_6 below 180 pptv and indicates air masses outside the plume. Dark grey and black is C_2H_6 above 180 pptv and represents plume air. Regions within the plume where ozone is above 70 ppbv are shaded black. Obviously high ozone mixing ratios are not distributed equally over the plume.

ACPD

7, 12067–12095, 2007

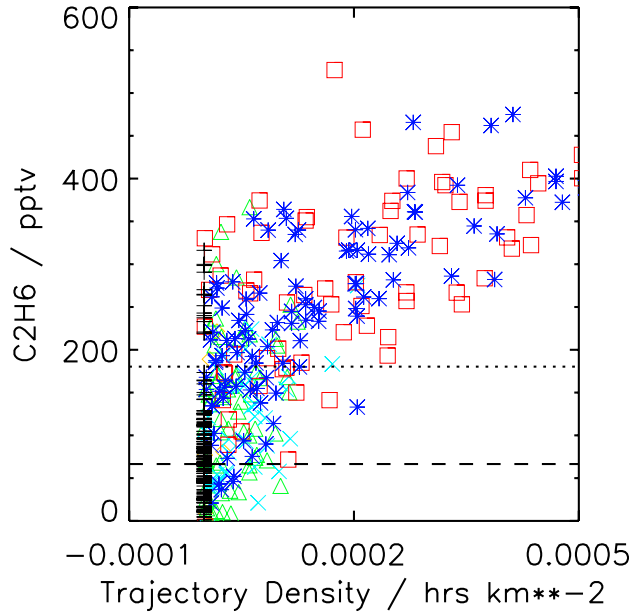

Fig. 10. C_2H_6 VMR over trajectory density. Trajectory density is the number of trajectories starting at biomass burning areas which touch a 5°×15° latitude-longitude bin, weighted by the time the trajectory is within the bin. The dashed line represents Southern hemispheric background C_2H_6, the dotted line is the plume threshold. Coloured symbols represent plume air. The trajectory origin is colour coded as in Fig. 9, i.e. light blue crosses: subtropical South America; red squares: Equatorial South America; yellow diamonds: North America; dark blue asterisks: Africa; green triangles: Australia, New Zealand. Black crosses represent air outside the plume.

ACPD
7, 12067–12095, 2007

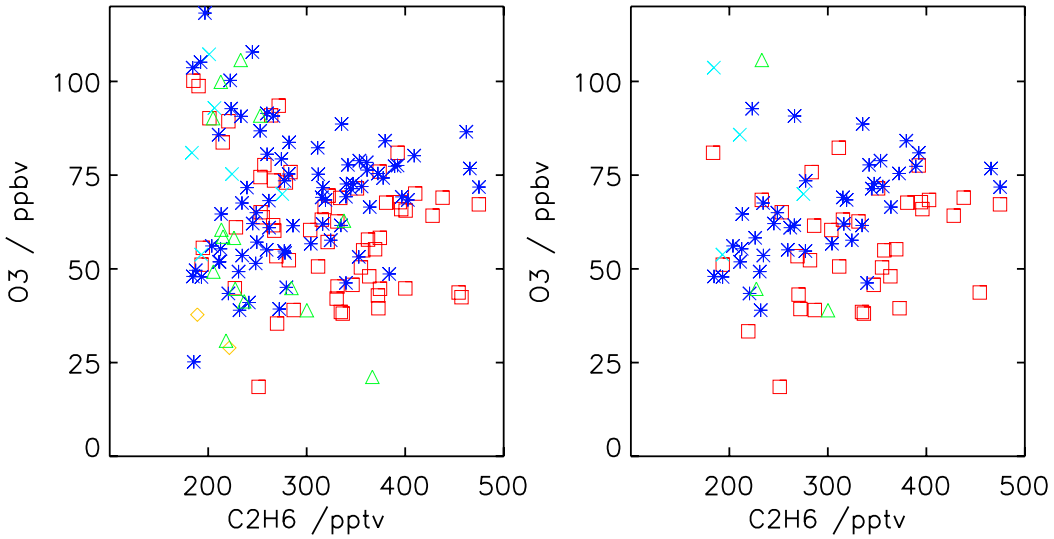

Fig. 11. O_3–C_2H_6 scatter plot. Colour coding as in Fig. 9. Left panel: The O_3/C_2H_6 ratio in the African part of the plume (dark blue asterisks) is higher than that of the tropical American part (red squares). No clear ozone/ethane correlation is evident within the plume. Also the Australian/Indonesian part of the plume (green triangles) contains data points of high ozone. Right panel: As above but data points with CFC-11 below 245 pptv, hinting at stratospheric signal, filtered out.

ACPD
7, 12067–12095, 2007

EGU